

Design of PI Tuning Controller using Genetic Algorithm for Load Frequency Control in Automatic Generation Control of Multi-Area Power System

J. Shankar¹, G. Mallesham², and Surender Reddy Salkuti³

^{1,2}Department of Electrical Engineering, University College of Engineering, Osmania University, Hyderabad, Telangana, India

³Department of Railroad and Electrical Engineering, Woosong University, Daejeon 34606 Korea

ABSTRACT:

Essentially, it is significant to supply the consumer with reliable and sufficient power. Since, power quality is measured by the consistency in frequency and power flow between control areas. The main objectives of load frequency control (LFC) are to regulate the electrical power supply in multi-area power system and change the system frequency and tie-line load. A number of modern control techniques are adopted to implement a reliable stabilizing controller. An attempt has been undertaken aiming at investigating the load frequency control problem in a power system consisting of the dynamic performance of Load Frequency Control (LFC) in three-area interconnected hydrothermal reheat and wind power system by the use of bio-inspired based algorithm. The performance of LFC has to be tuned properly so that its performance can be optimized. However, most of the tuning processes are performed through trial and error until the best performance is achieved. The proposed approach has superior feature, including easy implementation, stable convergence characteristics and very good computational performances efficiency. The main objective is to obtain a stable, robust and controlled system under 1%, 2% and 5% step load disturbance, by tuning the PI controller using Genetic algorithm (GA). The algorithm evaluates controller parameter using cost function such as Integral Time multiplied by Square Error (ITSE). The three-area interconnected power plant under consideration is implemented in MATLAB and simulation is carried out to get the optimum values of controller parameters. From simulation results obtained via Simulink (MATLAB), the frequency variations in each area, tie-line power fluctuation profile as well as the convergence trend for each algorithm has been analyzed in this paper. Besides various system parameters such as percentage overshoot, settling time, rise time and steady state error, different performance indices have also been computed. The experimental results demonstrated the comparison of the proposed system performance (GA-PI) with conventional controller of PI for the same investigated power system. The results proved that the GA based PI controller achieves better response than conventional PI controller.

Keywords: Proportional Integral (PI) Controllers, Genetic Algorithm (GA), Optimization Techniques, Area Control Error (ACE), Load Frequency Control, Load Interconnected system, Tie-Line Power and Automatic Generation Control (AGC)

1 INTRODUCTION:

In modern times, the growing population and rising demand for electricity make conventional sources of energy inadequate to meet the growth. Thus, tie lines are required to establish a connection between various independent conventional sources in order to tackle this problem. The loads could be shared amongst the various sources and could withstand changes in the power system with ease because to their interconnectedness. The frequency of the system is impacted even though there is a greater chance of benefit from connecting between various places when there is load variation. If the load varies or changes for whatever reason while the single energy source is operating, only that energy source's frequency is impacted. However, when many energy sources are operating, all variations in load in any part of the power system affect not just the frequency but also the power delivered across the tie line. Because the main controller previously depended on the governor's action to restore the system's operating frequency to its pre-disturbance value, there is still a steady state frequency error. Consequently, an additional controller is employed, which raises the system's order while eradicating the steady-state error. This controller is referred to as a secondary or integrated controller. Because it delivers electricity in a more reliable and improved form, LFC is essential to the functioning and management of the power system.

Restoring the system tie line power and frequency to their baseline levels before the disruption is one of LFC's most significant responsibilities. Controlling the generating units' usable power will help achieve this [1-4]. Everyone is aware of the continual fluctuations in the load during the day. During a power system's steady-state operation, kinetic energy

that is stored in the generator prime mover set modifies the load demand, resulting in a proportional shift in speed and frequency. A review and a state-of-the-art assessment of the AGC of power systems have been published in [5-6], respectively. There, several approaches to solving the AGC issue have been investigated. Thus, load frequency regulation is crucial to the electrical system's safe operation [7–10]. The most recent advancements in LFC techniques and methodology for various conventional and renewable energy-based power systems are thought to be found in the Automatic Generation Control (AGC).

It addresses both single- and multi-area power systems falling into these two groups. A power system ought to be regulated and restricted to a specific degree of deviation [11–15]. Better control strategies, including PID controllers combined with soft computing and optimization techniques, have been developed on automatic generation control (AGC) / load frequency control studies to increase transient responsiveness [16–20]. Control perspectives concerning frequency and power control have also been featured. The combined actions of unstructured and self-organized systems are known as swarm intelligence [21–25]. The major problem in any AGC, which has been addressed here, is frequency control. A proportional integral (PI) controller is optimized by a Genetic Algorithm (GA) for frequency management in an AGC-Multi Area structure which is exposed to fluctuations in addition to load changes [26-29].

2 THE COMPREHENSIVE THEORETICAL BASIS:

The Reheat thermal, wind, and hydroelectric components of the system have respective power outputs of 2000 MW, 35 MW, and 2000 MW. Through a tie line, these plants transfer power. To minimize framework and analytic approaches, models are constructed using a linear approach. A transfer function model for the wind power plant is created based on the assumption of a constant wind speed, and the wind power plant, which has a nominal rating of 35 MW, is further connected to the three Area Networks [30-31]. Figs. 4 and 5 depict the block diagram and pictorial representation of the connections between the three power systems. The list of various characteristics of a thermal-wind-hydropower system is displayed in Table 1. The three-area network is linked to a wind power facility with a nominal rating of 35 MW. It has long been assumed that wind farms are always in operation. There are three separate PI controllers in every system. For each of the three plants, transfer function models have been developed to do frequency response analysis. The Reheat thermal structure of the system was developed with consideration for the restrictions of both generating rate and reheat thermal [32–33]. The wind power system's transfer function model shows the hydro unit, the Wind Energy Conversion System (WECS), the generic speed governing system model, and the wind power plant constructed under the assumption of constant wind speed.

Table:1 Parameters of Simulated System

| Parametric Specifications of the Simulated Reheat Thermal and Hydro Power Plant | |
|--|-----------------------|
| P_r | 2000Mw |
| K_r | 0.5 |
| T_g | 0.08sec |
| T_t | 0.3sec |
| f | 50Hz |
| K_p | 120Hz/p. u Mw |
| T_r | 10sec |
| $P_{tie\ max}$ | 200Mw |
| T_p | 20sec |
| H | 5 sec |
| P_r | 35 Mw |
| D | 0.00833 p.u. Mw/Hz |
| R | 2.4 Hz/p.u. Mw |
| Parametric Wind Power Plant Simulation Specifications | |
| Density of Air | 1.2 kg/m ³ |
| Gear ratio | 70 |

| | |
|-------------------------|--------|
| T _{pt} | 10.55 |
| Radius of turbine blade | 45m |
| K _{pt} | 0.012 |
| H | 5 sec |
| Average wind velocity | 7m/s |
| T _i | 3 sec |
| T _p | 20 sec |
| T ₁₂ | 0.544 |

2.1 Thermal Power Station:

The highly pressurized steam in a thermal power plant is used to recover thermal potential energy, which is then used to power a generator. The first unit in the Simulink model in Fig. 1 is the governor, which regulates the quantity of steam that enters the turbine. The following is a representation of a governor's transfer function:

$$G_{gt}(s) = \frac{K_g}{T_g \cdot s + 1} \tag{1}$$

The turbine expands with the pressurized steam that enters through a steam inlet valve. The transfer function of the steam turbine can be represented as follows:

$$G_{Tt}(s) = \frac{K_t}{T_t \cdot s + 1} \tag{2}$$

The Steam exhaustion and an increase in moisture content are caused by the expansion of steam inside a turbine. Consequently, in order to remove any remaining moisture, the steam produced by the steam turbine needs to be heated again. A common approach to express the transfer function of a conventional re-heater is as

$$G_{Rh}(s) = \frac{K_r \cdot T_r \cdot s + 1}{T_r \cdot s + 1} \tag{3}$$

The turbine is mechanically coupled to an electric generator. Such a generator's transfer function can be expressed as follows:

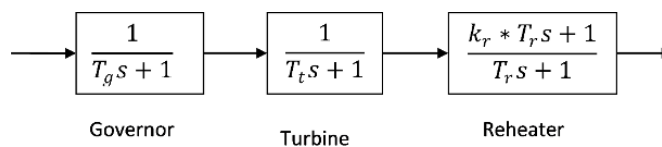


Fig.1 Mathematical Modeling of Reheat Thermal Power station

2.2 Hydro Power Station:

Water is kept in hydroelectric power plants to a height known as the "head." When the dammed water is forced to flow downward via the penstock and into the turbine, its potential energy is transformed into kinetic energy, which powers the turbine to produce electricity. The hydro governor is the initial block in the Simulink model of a hydroelectric power plant of Fig.2. A hydroelectric plant governor's transfer role can be expressed as follows:

The hydraulic turbine's transfer function is

$$G_{Ht}(s) = \frac{-T_w \cdot s + 1}{0.5T_w \cdot s + 1} \tag{4}$$

Transfer function of hydraulic Governor is,

$$\frac{K_d \cdot s^2 + K_p \cdot s + K_i}{K_d \cdot s^2 + \left(K_p + \frac{f}{R_2}\right) s + K_i} \tag{5}$$

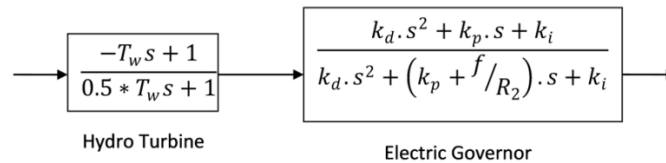


Fig.2 Mathematical Modeling of Hydro Power station

2.3 Wind Energy Conversion System:

The two-pole-one-zero transfer function illustrated below can be used to explain the dynamic operation of the Wind Energy Conversion System (WECS): Wind Energy Conversion System (WECS) natural frequencies and damping ratios are determined by the poles of the transfer function, where T_e and T_{pt} are the parasitic and main time constants, respectively. It adds new dynamics, like oscillations, settling time, and overshoot, that might affect how the system behaves. The mathematical model block in Fig. 3's Simulink model that represents a wind turbine plant is the WECS.

By choosing the suitable natural frequency ω_n and damping factor γ , the wind energy conversion system's second-order dynamics may be obtained, which in turn provides the controller settings.

$$T_i = \frac{2\gamma}{\omega_n} - \frac{1}{\omega_n^2 T_{pt}} \tag{6}$$

$$K_p = \left(\frac{T_i T_p}{K_{pt}}\right) \omega_n^2 \tag{7}$$

$$H_{pt}(s) = \frac{K_{pt}(T_{zs} + 1)}{(T_{es} + 1)(T_{pt} + 1)} \tag{8}$$

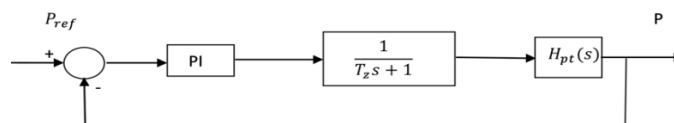


Fig.3 Mathematical Modeling of WECS

The Integral Time Square Error (ITSE) was chosen as the performance index, which can be written as:

$$ITSE = \int \left\{ (\Delta f_i)^2 + (\Delta P_{tie_{i-j}})^2 \right\} t \cdot dt. \tag{9}$$

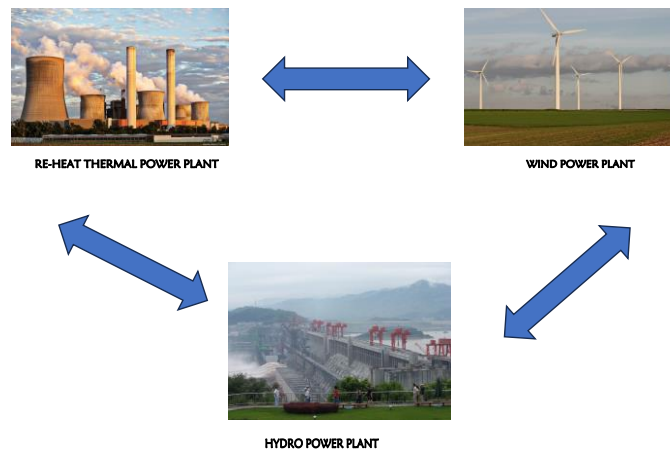


Fig.4 A graphical representation of three distinct yet linked regions via a tie-line

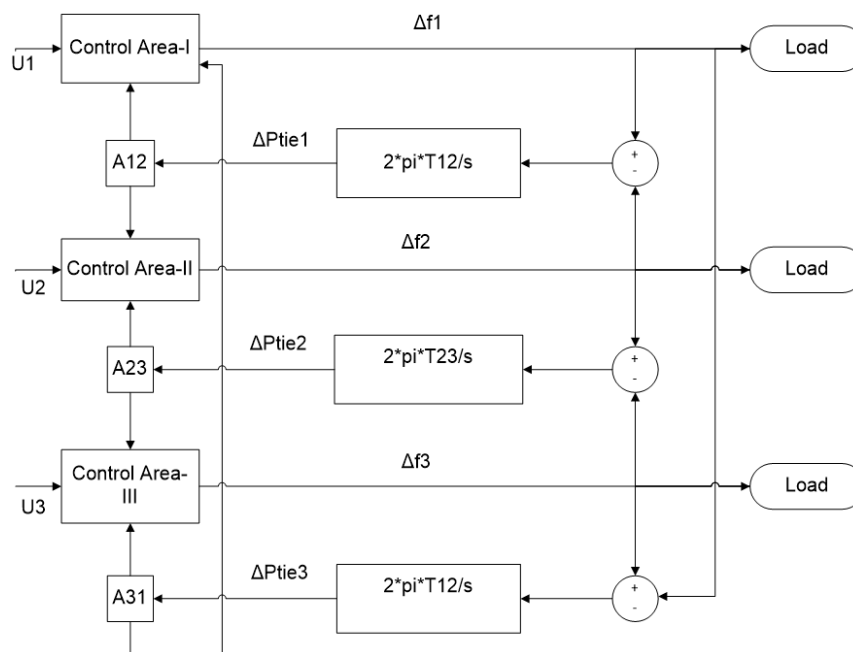


Fig.5 Block schematic illustration of a three-area system which is interconnected

3 CONTROL METHODOLOGY

3.1 Proportional Integral (PI) Controller

Through the mitigation of the individual's disadvantages, the PI controller is utilized, which combines the benefits of the integral and proportional controllers. Equation (10) provides the conventional PI controller's transfer function, where K_p and K_i stand for the controller's parameters.

$$H(s) = \frac{U(s)}{E(s)} = K_p + \frac{K_i}{s} \tag{10}$$

Equation (11) also illustrates the PI controller's time domain representation. where the error-caused response, $u(t)$, is given by $e(t)$.

$$U(t) = K_p + K_i \int e(t)dt \tag{11}$$

3.2 GENETIC ALGORITHM (GA)

Genetic Algorithm (GA) is a computational abstraction of natural evolution that can be used to solve some optimization problems proposed by Holland in 1975. It is a repetitive search procedure that operates on a set of strings called chromosomes. The implementation of this algorithm is briefly listed in the following process [34-36]. GA solves optimization problems by exploitation of random search. When searching a large space GA may offer significant benefits over the traditional optimization techniques. In this problem GA is used to optimize the gains of conventional PI controller performance index as fitness functions.

Here, addresses to employ an optimal PI controller for frequency regulation of AGC system, the main issues are tuning the optimal values to solve by GA through an objective function [Eq. (9)]. PI tuned GA controller automatically specified with objective functions, which is formulated and calculate the controller’s performance in terms of time-domain bounds on the response of closed-loop. A GA (shown in Fig. 8) has enhanced the appearance of the computer system and works without detail. It depends on the evolutionary operators’ reactions such as reproduction, cross-over, and mutation. Within a GA, the issue is investigated and initialized by population, development, exercise measurement, population fitness selection, and reproduction and provides the best solution fitness.

Reproduction: creates new generation of chromosomes, fitness proportionate reproduction is achieved through roulette wheel selection.

Crossover: allows information to be exchanged between individuals in the population. Two parent strings are selected randomly and a new child string is created by combining random sub-string from two parent strings.

Mutation: random alteration of bits in a string which flips a bit from 1 to 0 or vice versa. By the end of mutation new generation is complete and process is repeated for evaluation of new fitness.

- ✚ Initialize the chromosome strings of population.
- ✚ Decode the strings and assess them.
- ✚ Choose the best strings.
- ✚ Copy the best strings and paste them on the non-selected strings.
- ✚ Combine and develop it to generate off strings.
- ✚ Update the genetic cycle and stop the process. The values of GA parameters are set according to table 2.

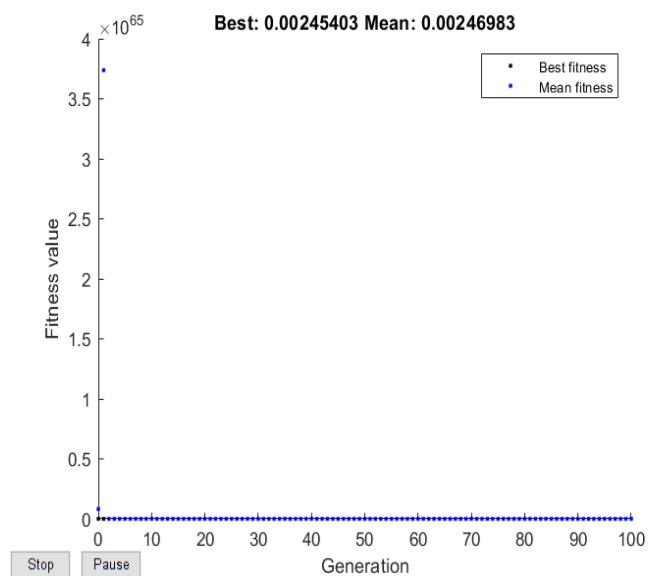
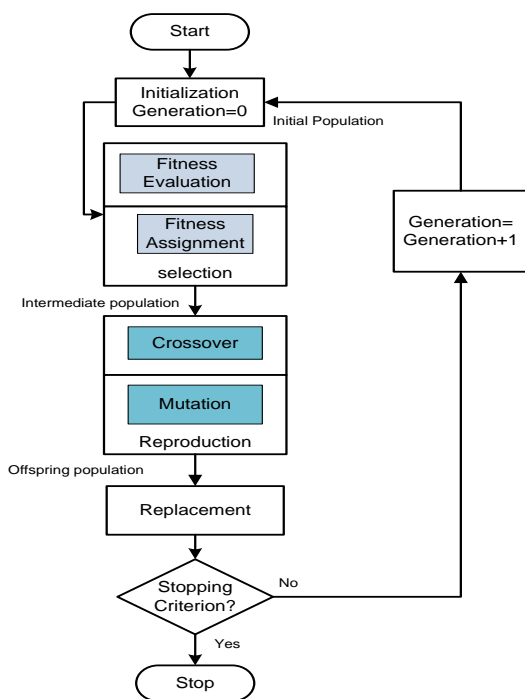


Table:2 GA Simulation Parameters

| GA Parameters | |
|------------------------------------|-----|
| Population size | 50 |
| Problem dimension | 6 |
| Number of generations | 100 |
| Decision variable boundaries (min) | 0.7 |
| Decision variable boundaries (max) | 0.2 |

4 RESULTS AND DISCUSSION

The optimization issues, PI Controllers, and load frequency regulation received a lot of attention. It is well known that the power system maintains system parameters within permissible bounds and can sustain its load while operating normally. On the other side, the system variables are impacted by an abrupt breakdown in the power system. Controllers must be utilized to overcome this issue. The principal control loop of a power system is considered an extra controller. Utilizing the error signal from the power system, the PI controller—which functions as a secondary controller in the current study—calculates the proper control signal to generate.

Frequency Responses: To demonstrate the improvements, a single area (Area 1) is chosen for both models and the GA optimized PI controller's frequency response (bold line) is represented in table with the Default PI controller's frequency characteristics. As can be seen from Figures 6, 8 and 10 GA optimized PI controller has lower deviations from the nominal frequency value (50Hz). The system's frequency becomes steady, from the load disturbances of 1%, 2% and 5% whereas the default PI controller has a more prominent undershoot and overshoot steady-state error and settling time to its frequency characteristics. It also becomes stable much later than the GA-optimized controller.

Tie-line Control: When we take a look at the tie-line power exchange between areas 1 and 3, the GA optimized PI controller affected the system. It proves that the tuned controller remarkably eliminated the initial oscillations and also greatly improved the overshoot and undershoot characteristics of the tie-line power exchange signal. The exchange between areas stopped much earlier, whereas the default PI controller performed not upto the mark in all the aforementioned signal characteristics. The controller of the model imposed showed much less improvement in initial oscillations when tuned with the proposed GA but the characteristic of the signal got almost totally eliminated with less time required to cease the tie-line power exchange between areas 1 and 3 compared to the default PI controller. This can be observed in Figures 6, 8 10.

The power system uses the control signal that the controller generates as a reference signal. The system frequency and tie-line power flow error-connected associated regions are combined linearly to form the error signal. Thus, a multi-area reheat power system was planned and implemented using the MATLAB/Simulink environment, and it was examined in this work. To assess the superior performance of the suggested method, a PI controller and step load perturbations (SLPs) of 1%, 2%, and 5% in Area 1 are employed to simulate the necessary power system. An independent MATLAB file contains the optimization algorithm that is developed and used to modify the controller's parameters. In this simulated scenario, the GA method is considered for optimizing the gain values of the controller parameters.

4.1 1% Step Load Disturbance in Area-1

In this Scenario The recommended controllers are applied to a 0.01 percent increase in load demand across the three regions in MATLAB/Simulink to mimic the recommended model. Figures 6 and 7 depict, respectively, the frequency variations, Tie-line power variations, and Area Control Error fluctuations of the Reheat thermal area, wind area, and hydropower area for the system dynamic reactions. The GA-tuned controller has a quicker settling time than the conventional PI controller, but it has better peak overshoots and peak undershoots. In the end, the developed controller outperforms the other controllers in terms of dynamic responsiveness. With these factors and dynamic reactions in mind, the power transfer deviation via the tie line, frequency offset, and Area Control Error were computed at each of the three locations. As a result, for the closed-loop system, the observed system responses, tie-line power flow, and area control errors are displayed in Figs. 6 and 7. The suggested GA-PI Controller has a substantially shorter settling time and overshoots than the traditional PI controller.

Figures 6 and 7 for the frequency variations, tie-line power, and area control error all clearly show this. It is clear that, in comparison to the other areas, area-1's frequency deviation has the largest undershoot peak. In contrast to the other areas, it has the least amount of overshoot peak. When compared to the other areas of the values, area-1 exhibits a positive overshoot peak in relation to the tie-line power flow. As a result, the recommended GA-PI controller outperforms the conventional PI Controller for the Multi Area Power System. A summary of the controllers' gains is shown in table 3.

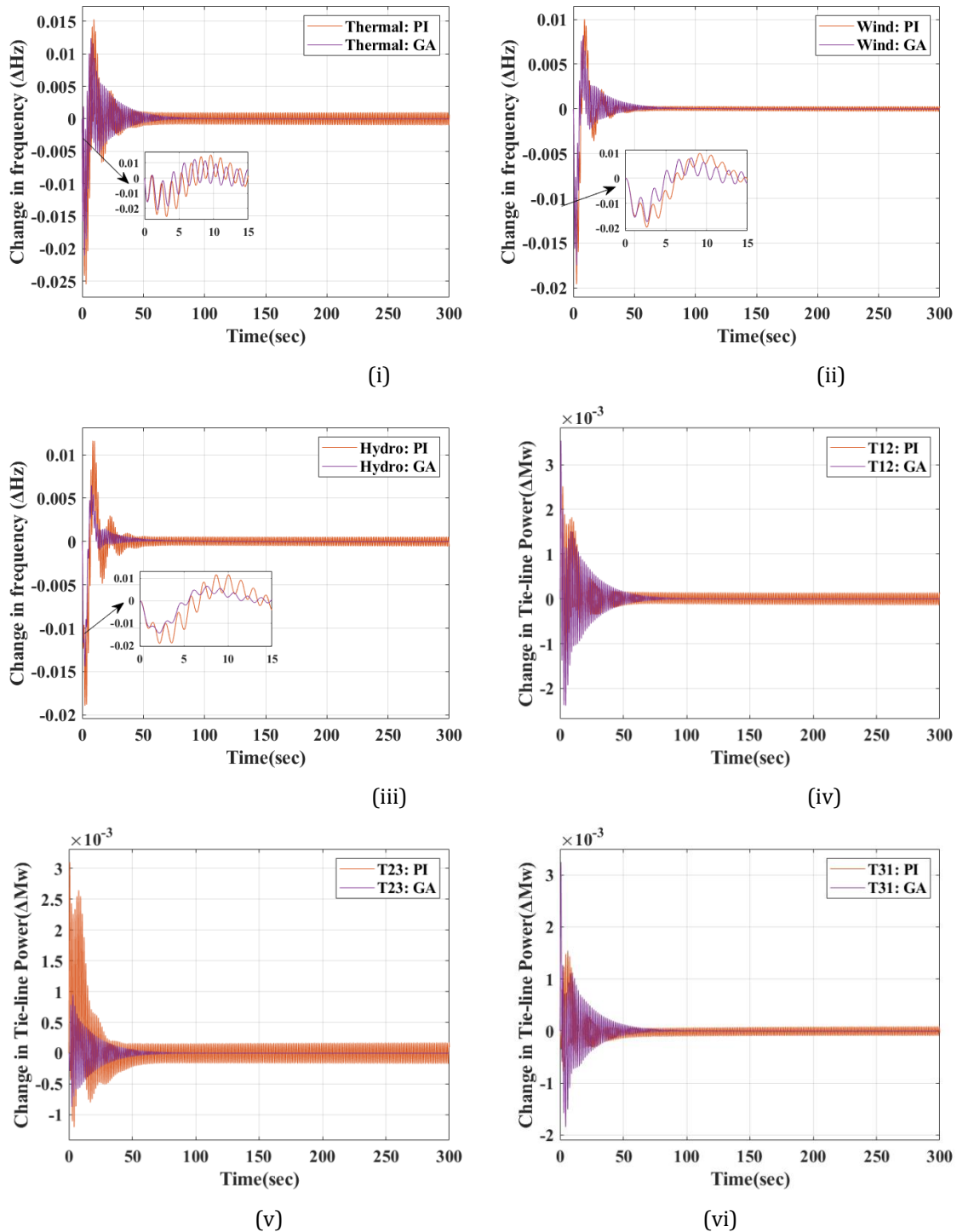
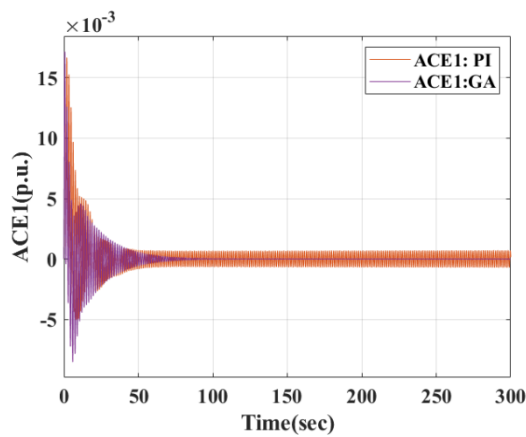
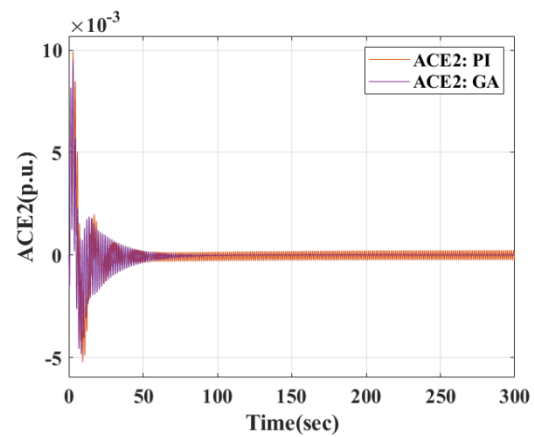


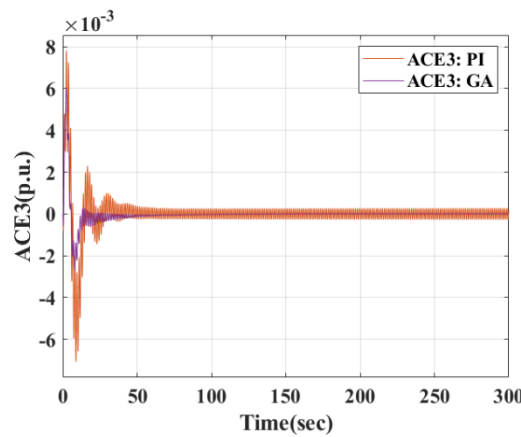
Figure 6: Evaluation of 1% Change in load in AREA-1; (i) Variations in Area-1 frequency, (ii) Variations in Area-2 frequency, (iii) Variations in Area-3 frequency, and (iv) Variations in Area-1 and Area-2 Tie-Line Power (v) Variation in Area-2 and Area-3 Tie-Line Power (vi) Variation in the Tie-Line Power between Areas 1 and 3



(vii)



(viii)



(ix)

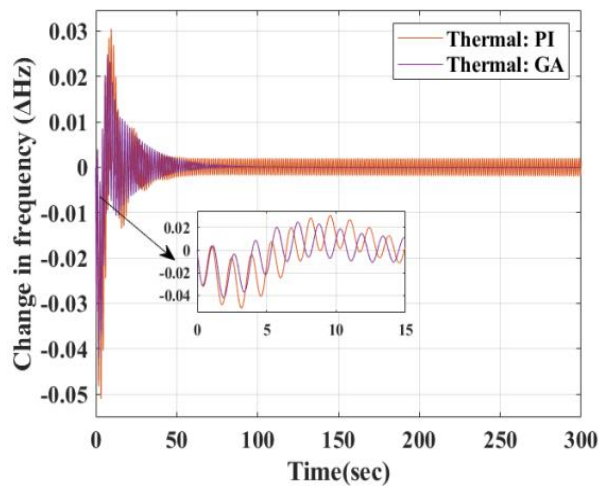
Fig.7. The attainment of a 1% Change in load in AREA-1; Area Control Errors for Areas 1 through 3 are shown in (vii), (viii), and (ix) respectively.

Table:3 Steady State Error, Peak Under Shoot, Peak Over Shoot, and Settling Time Comparison Values for 1% Variation Load in Area-1

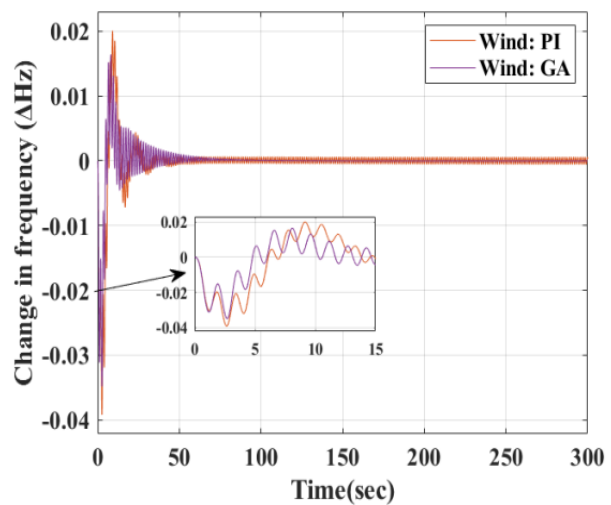
| | STEADY STATE ERROR | | PEAK OVER SHOOT | | PEAK UNDER SHOOT | | SETTLING TIME | |
|-------------------|--------------------|--------------------|-----------------|------------------|--------------------|------------------|---------------|------------|
| | PI | GA | PI | GA | PI | GA | PI | GA |
| ΔF_1 | 0.0006213 | -0.00001448 | 0.01533 | 0.01241 | -0.025451 | -0.02091 | Oscillate | 120 |
| ΔF_2 | 0.0001396 | -0.00001450 | 0.01002 | 0.00823 | -0.019499 | -0.01738 | Oscillate | 110 |
| ΔF_3 | -0.0005511 | -0.00001460 | 0.01164 | 0.006487 | -0.018973 | -0.01434 | Oscillate | 100 |
| ΔP_{tie1} | 0.0006213 | -0.00001448 | 0.003364 | 0.003536 | -0.0014492 | -0.002345 | Oscillate | 145 |
| ΔP_{tie2} | 0.0001396 | -0.00001450 | 0.001546 | 0.0009541 | -0.00076913 | -0.0008439 | Oscillate | 115 |
| ΔP_{tie3} | -0.0005511 | -0.00001460 | 0.003100 | 0.003246 | -0.0012029 | -0.0001839 | Oscillate | 115 |
| ACE_1 | 0.0006213 | -0.00001448 | 0.01668 | 0.01718 | -0.0050127 | -0.008507 | Oscillate | 135 |
| ACE_2 | 0.0001396 | -0.00001450 | 0.009926 | 0.009463 | -0.0052024 | -0.004742 | Oscillate | 130 |
| ACE_3 | -0.0005511 | -0.00001460 | 0.007814 | 0.006014 | -0.0071068 | -0.002595 | Oscillate | 115 |

4.2 2% Step Load Disturbance in Area-1

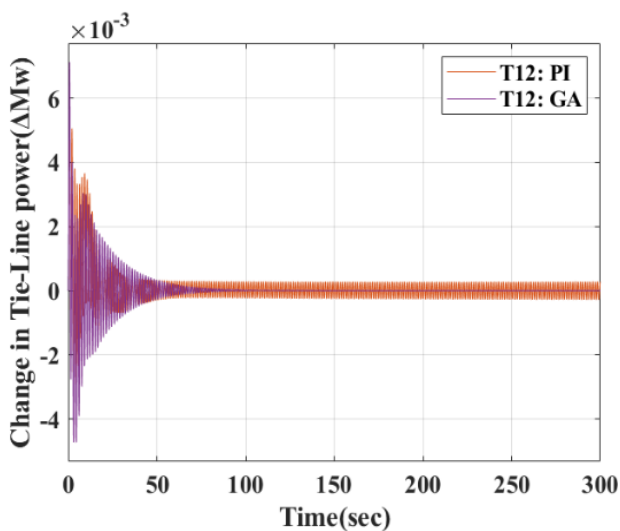
In this Situation To observe the robustness of the system, the given model is simulated in MATLAB/Simulink with the suggested controllers applied to a 0.02 percent increase in load demand across the three areas. Figs. 8 and 9 show the frequency deviations, Tie-line power flow, and Area Control Error for the Reheat thermal zone, wind area, and hydro region, respectively, which reflect the system dynamic responses. The GA-PI Controller has better peak overshoots and peak undershoots as well as steady state even though it settles faster than the PI controller. Table 4 displays the frequency deviation, tie-line power deviations, and area control error for the wind, hydro, and reheat thermal zones, respectively, as indicators of the system dynamic reactions. The GA-PI Controller outperforms the PI Controller in terms of steady state error, peak overshoots, and peak undershoots, even though it settles faster. In terms of dynamic reactivity, the designed controller finally performs better than the other controllers.



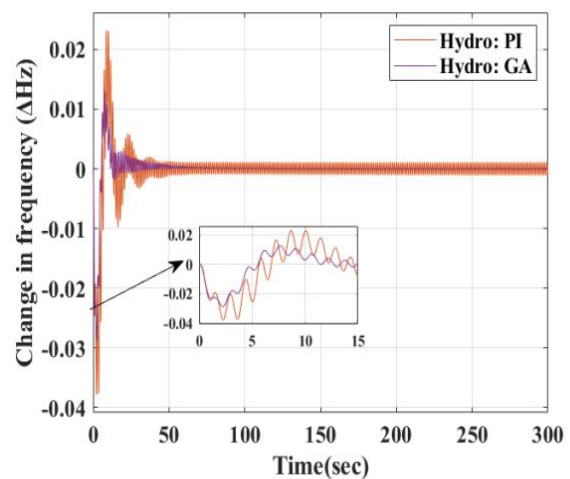
(i)



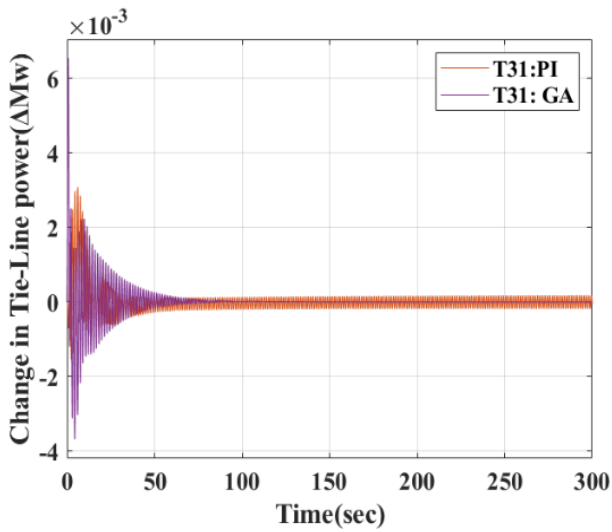
(ii)



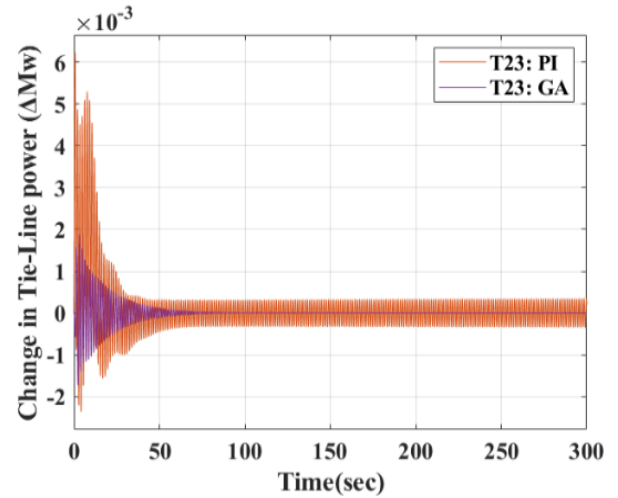
(iii)



(iv)

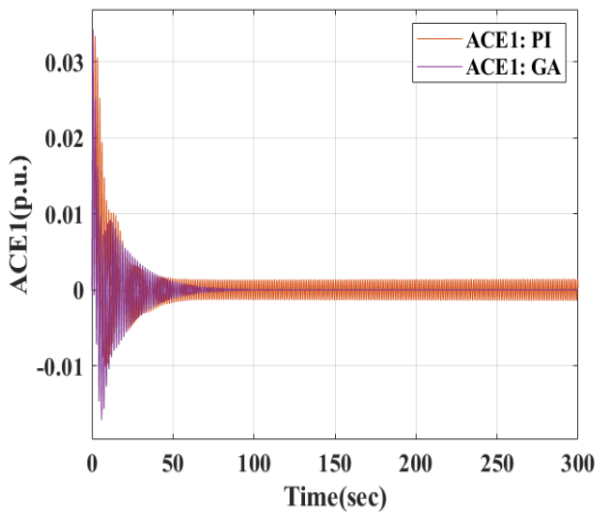


(v)

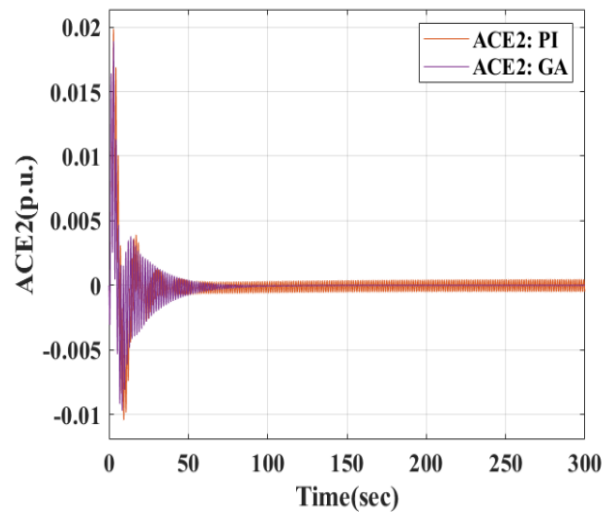


(vi)

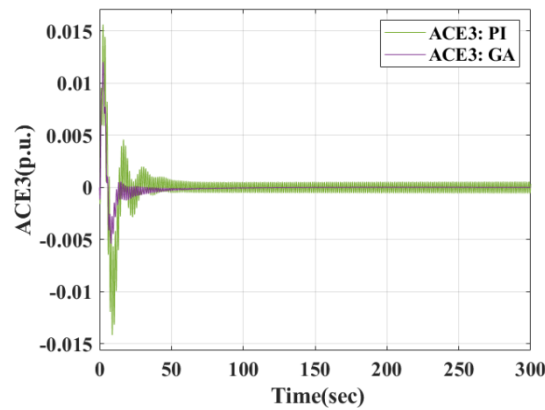
Fig. 8. Evaluation of 2% Change in load in AREA-; (i) Variations in Area-1 frequency, (ii) Variations in Area-2 frequency, (iii) Variations in Area-3 frequency, and (iv) Variations in Area-1 and Area-2 Tie-Line Power (v) Tie-line power change between Area-2 and Area-3 (vi) Tie-line power change between Area-3 and Area-1;



(vii)



(viii)



(ix)

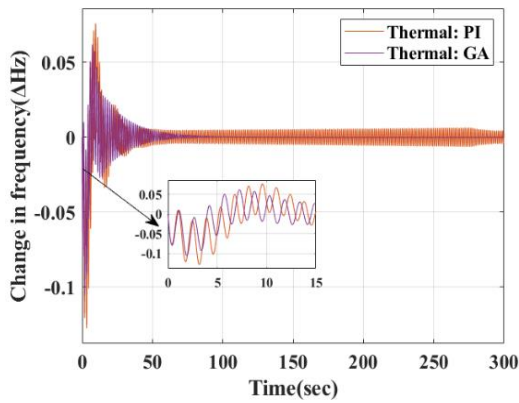
Fig.9. The attainment of a 2% Change in load in AREA-1; Area Control Errors for Areas 1 through 3 are shown in (vii), (viii), and (ix) respectively.

Table:4 Comparison values of Steady State Error, Peak Over Shoot, Peak Under Shoot and Settling Time for 2% Change Load in Area-1

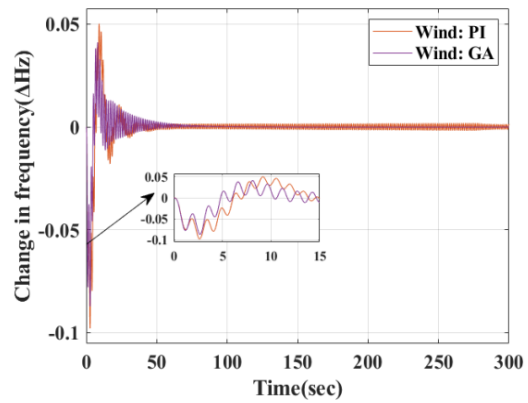
| | STEADY STATE ERROR | | PEAK OVER SHOOT | | PEAK UNDER SHOOT | | SETTLING TIME | |
|-------------------|--------------------|--------------------|-----------------|-----------------|-------------------|------------------|---------------|------------|
| | PI | GA | PI | GA | PI | GA | PI | GA |
| ΔF_1 | 0.001277 | -0.00002896 | 0.03051 | 0.02487 | -0.0511 | -0.04201 | oscillate | 120 |
| ΔF_2 | 0.0002779 | -0.00002899 | 0.02006 | 0.01639 | -0.039221 | -0.03480 | oscillate | 110 |
| ΔF_3 | -0.001118 | -0.00002919 | 0.02316 | 0.01300 | -0.037869 | -0.02867 | oscillate | 100 |
| ΔP_{tie1} | 0.001277 | -0.00002896 | 0.006693 | 0.007193 | -0.0029186 | -0.004715 | oscillate | 145 |
| ΔP_{tie2} | 0.0002779 | -0.00002899 | 0.003085 | 0.001886 | -0.0015401 | -0.001669 | oscillate | 115 |
| ΔP_{tie3} | -0.001118 | -0.00002919 | 0.006221 | 0.006541 | -0.0023506 | -0.003669 | oscillate | 115 |
| ACE_1 | 0.001277 | -0.00002896 | 0.03340 | 0.03431 | -0.010006 | -0.01700 | oscillate | 135 |
| ACE_2 | 0.0002779 | -0.00002899 | 0.01985 | 0.01891 | -0.010433 | -0.009470 | oscillate | 130 |
| ACE_3 | -0.001118 | -0.00002919 | 0.01563 | 0.01204 | -0.014126 | -0.005192 | oscillate | 115 |

4.3 5% Step Load Disturbance in Area-1

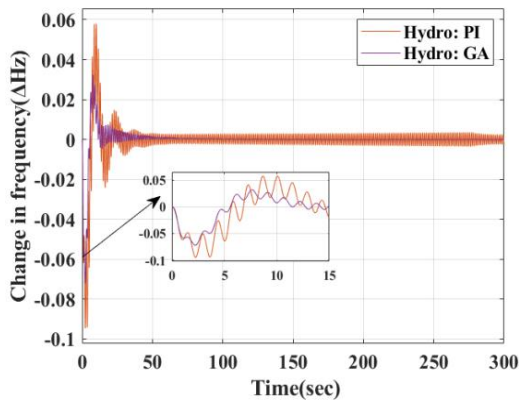
In this case, to observe the robustness of the system, the given model is simulated in MATLAB/Simulink with the suggested controllers applied to a 0.02 percent increase in load demand across the three areas. Figs. 10 and 11 show the frequency deviations, Tie-line power flow, and region Control Error for the Reheat thermal zone, wind region, and hydro area, respectively, which reflect the system's dynamic responses. The GA-PI Controller has better peak overshoots and peak undershoots as well as a steady state, even though it settles faster than the PI controller. Table 5 displays the frequency deviation, tie-line power deviations, and area control error for the wind, hydro, and reheat thermal zones, respectively, as indicators of the system's dynamic reactions. The GA-PI Controller outperforms the PI Controller in terms of steady-state error, peak overshoots and undershoots, and settling time. In terms of dynamic reactivity, the designed controller finally performs better than the other controllers.



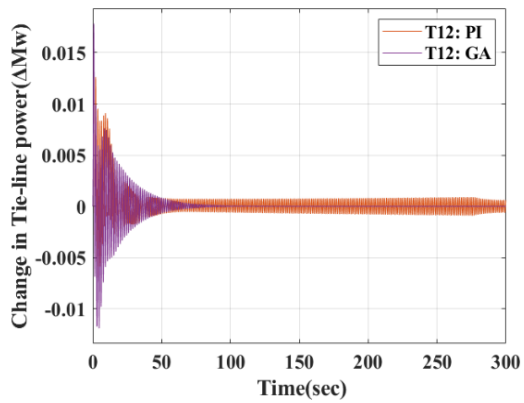
(i)



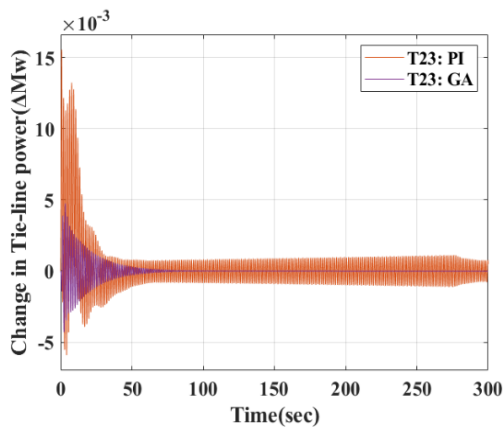
(ii)



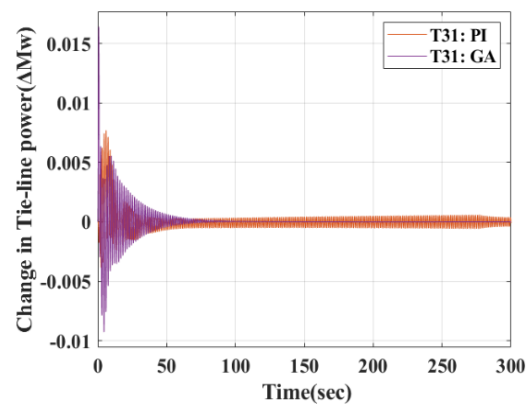
(iii)



(iv)

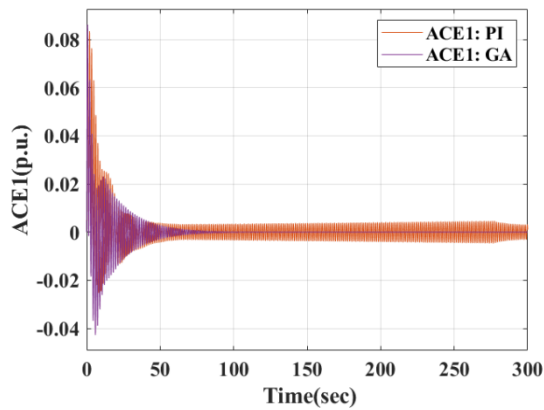


(v)

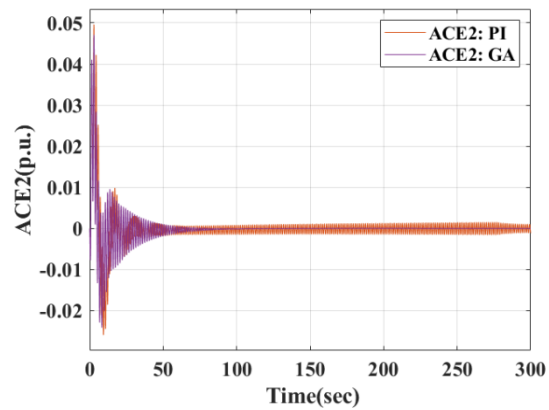


(vi)

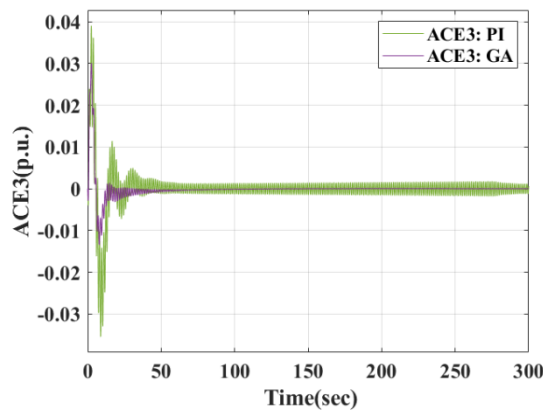
Fig.10. Evaluation of 5% Change in load in AREA-1; (i) Variations in Area-1 frequency, (ii) Variations in Area-2 frequency, (iii) Variations in Area-3 frequency, and (iv) Variations in Area-1 and Area-2 Tie-Line Power (v) Tie-line power change between Area-2 and Area-3 (vi) Tie-line power change between Area-3 and Area-1;



(vii)



(viii)



(ix)

Fig.11. The attainment of a 5% Change in load in AREA-1; Area Control Errors for Areas 1 through 3 are shown in (vii), (viii), and (ix) respectively.

Table:5 Comparison values of Steady State Error, Peak Over Shoot, Peak Under Shoot and Settling Time for 5% Change Load in Area-1

| | STEADY STATE ERROR | | PEAK OVER SHOOT | | PEAK UNDER SHOOT | | SETTLING TIME | |
|-------------------|--------------------|--------------------|-----------------|-----------------|-------------------|-----------------|---------------|------------|
| | PI | GA | PI | GA | PI | GA | PI | GA |
| ΔF_1 | 0.002374 | -0.0000724 | 0.07585 | 0.06200 | -0.12809 | -0.01507 | oscillate | 120 |
| ΔF_2 | 0.000762 | -0.00007249 | 0.05022 | 0.04118 | -0.097826 | -0.08724 | oscillate | 110 |
| ΔF_3 | -0.002481 | -0.00007299 | 0.05800 | 0.03249 | -0.094467 | -0.07159 | oscillate | 100 |
| ΔP_{tie1} | 0.002374 | -0.0000724 | 0.01679 | 0.01783 | -0.0072912 | -0.01190 | oscillate | 145 |
| ΔP_{tie2} | 0.000762 | -0.00007249 | 0.007703 | 0.004762 | -0.0038855 | -0.004296 | oscillate | 115 |
| ΔP_{tie3} | -0.002481 | -0.00007299 | 0.01556 | 0.01641 | -0.0059212 | -0.009193 | oscillate | 115 |
| ACE_1 | 0.002374 | -0.0000724 | 0.08348 | 0.08623 | -0.025303 | -0.04221 | oscillate | 135 |
| ACE_2 | 0.000762 | -0.00007249 | 0.04961 | 0.04710 | -0.025971 | -0.02373 | oscillate | 130 |
| ACE_3 | -0.002481 | -0.00007299 | 0.03907 | 0.03012 | -0.035398 | -0.01300 | oscillate | 115 |

5 CONCLUSION AND FUTURE SCOPE

The design of Load Frequency Control (LFC) for multi-area Thermal-Wind-Hydro power systems is presented in this study. When there is a disruption in the load, control performance is improved by using a proportional integral (PI) controller. The PI Controller's gain settings are optimized by experimenting with the ITSE objective function. In the Reheat thermal area (Area 1), the efficacy of the PI controllers is analyzed and compared for 1%, 2%, and 5% Step Load interruption. The aforementioned system employs an optimized integrated controller for its AGC in the event of an abrupt disruption in load. The type of controller plays a role in the performance of the LFC system. PI controller yields the best performance but introduces more parameters to be optimized and hence increases the complexity in terms of optimization. Utilizing GA allows us to solve high-order, nonlinear problems without worrying much about the number of variables. Due to the GA nature, introducing multiple variables is possible and the algorithm will iterate over each variable according to the parameters that it is set to run.

No matter the controller type and the optimization technique, the LFC system's frequency response was much better. When PI Controller is imposed, it takes the system a long time to regain the nominal frequency, and also the frequency value deviates much more during the transient state compared to the system. The regular controllers may or may not show sufficient results in regaining the nominal system frequency within the desired time limit or damping the oscillations during and after the external disturbances. Most papers considering GA application is LFC do have a high number of populations is sizes with a high number of iterations as termination conditions. In this paper, results have been obtained with much less population size and with fewer iterations. Utilizing GA allows the system to react much quicker to such disturbances, lower settling time, and increase the undershoot and overshoot parameters of the frequency.

ITSE has been introduced as the cost function have been executed to select the best I AE value-bearing GA run. This greatly affects the required time for a GA run to complete and the parameters selected for the GA yielded sufficient with different load conditions. The algorithm presented in this paper can be utilized to obtain better optimized PI controller gains in a much shorter time for GA applications. Comparisons between PI and GA-PI controllers are used in order to better optimize the gain values of PI controllers. When compared to the power system response equipped with a standard PI controller, it is shown that the GA-PI controller efficiently reduces the electromechanical oscillations, settling time, steady state error, peak over, and undershoots. by using several improved algorithms to include additional renewable energy sources into the linked power system problem.

NOMENCLATURE

| THREE AREA SYSTEM Parameters | |
|------------------------------|--|
| T_g | Time Constant of Governor |
| T_t | Time Constant of Turbine |
| T_r | Time Constant of Reheater Thermal Power |
| T_w | Water Time Constant |
| K_p | the electric governor proportional gain |
| U_1 | Control outputs from Area-1's controller |
| U_2 | Control Outputs from Area-2's controller |
| U_3 | Control Outputs from the controller of Area-3 |
| A_{12} | Constants for synchronizing coefficients of Tie-Line-1 |
| A_{23} | Constants for synchronizing coefficients of Tie-Line-2 |
| A_{31} | Constants for synchronizing coefficients of Tie-Line-3 |
| ΔP_{tie12} | Incremental shift in tie line power of Tie-Line-1 |
| ΔP_{tie23} | Incremental shift in tie line power of Tie-Line-2 |
| ΔP_{tie31} | Incremental shift in tie line power of Tie-Line-3 |
| T_{12} | Coefficient of synchronization of Tie-Line-1 |
| T_{23} | Coefficient of synchronization of Tie-Line-2 |

| | |
|--------------|--|
| T_{31} | Coefficient of synchronization of Tie-Line-3 |
| Δf_1 | Deviations in system frequency in Area-1 |
| Δf_2 | Deviations in system frequency in Area-2 |
| Δf_3 | Deviations in system frequency in Area-3 |
| K_g | Gain value of Governor |
| K_t | Gain Value of Turbine |
| K_r | Coefficient of reheat steam Turbine Constant |
| K_d | the electric governor derivative gain |
| K_i | the electric governor integral gains |
| T_ϵ | the parasitic time constant |
| T_{pt} | the main time constant |

6 REFERENCES

- [1]. N.E.Y. Kouba, M. Mena, M. Hasni, M. Boudour, Load Frequency Control in multi-area power system based on Fuzzy Logic-PID Controller, in 2015 IEEE International Conference on Smart Energy Grid Engineering (SEGE), Oshawa, ON, Canada, 2015.
- [2]. Dola Gobinda Padhan, Somanath Majhi, "A new control scheme for PID load frequency controller of single-area and multi-area power systems", ISA Transactions, Volume 52, Issue 2, 2013, Pages 242-251, ISSN 0019-0578,
- [3]. D. H. Tungadio and Y. Sun, "Load frequency controllers considering renewable energy integration in power system," Energy Reports, 2019, vol. 5, pp. 436–453.
- [4]. Asma Aziz, Aman Than Oo, Alex Stojcevski, "Analysis of frequency sensitive wind plant penetration effect on load frequency control of hybrid power system", International Journal of Electrical Power & Energy Systems, vol.99, pp.603-617, July 2018.
- [5]. Sarker, Md, Hasan, Kamrul. "Load Frequency Control in Power System". 10. 23-30. 2016.
- [6]. K. Jagatheesan and B. Anand, "Automatic generation control of three area hydro-thermal power systems with electric and mechanical governor," IEEE International Conference on Computational Intelligence and Computing Research, Coimbatore, India, 2014, pp. 1-6.
- [7]. Kothari D. P., Nagrath I.J., 2003. Modern Power System Analysis, Tata Mc Gro Hill, Third Edition.
- [8]. Wadhawa C.L., 2007. "Electric Power System" New Age International Pub. Edition.
- [9]. Elgerd O. I. 1971. Electric Energy System Theory; An Introduction, Mc Gro Hill.
- [10]. Z. A. Obaid, L. M. Cipcigan, L. Abraham, and M. T. Muhssin, "Frequency control of future power systems: reviewing and evaluating challenges and new control methods," J. Mod. Power Syst. Clean Energy, 2019, vol. 7, no. 1, pp. 9–25.
- [11]. D. K. Gupta, R. Naresh and A. V. Jha, "Automatic Generation Control for Hybrid Hydro-Thermal System using Soft Computing Techniques," 2018 5th IEEE Uttar Pradesh Section International Conference on Electrical, Electronics and Computer Engineering (UPCON), Gorakhpur, 2018, pp. 1-6.
- [12]. P. Anil Kumar, J. Shankar "Dynamic Analysis and Stability of the Load Frequency Control in Two Area Power System with Steam Turbine" having ISSN: 2248-9622 Vol. 2, Issue 6, November- December 2012, pp.1573-1577.

- [13]. Abdul Latif, S.M. Suhail Hussain, Dulal Chandra Das, Taha Selim Ustun, "State-of-the-art of controllers and soft computing techniques for regulated load frequency management of single/multi-area traditional and renewable energy-based power systems, *Applied Energy*, Volume 266, 2020, 114858, ISSN 0306-2619
- [14]. M. Suman, M. Venu Gopala Rao, G. R. S. Naga Kumar and O. Chandra Sekhar, "Load frequency control of three-unit interconnected multimachine power system with PI and fuzzy controllers," 2014 International Conference on Advances in Electrical Engineering (ICAEE), Vellore, 2014, pp. 1-5.
- [15]. Tshinavhe, Ntanganedzeni Ratshitanga, Mukovhe, Tsheme, Nomzamo. Review of Adaptive Load Frequency Control Strategies for Improving Wind Power Plant Integration, 2024, pp 1-6.
- [16]. Irfan Ahmed Khan, Hazlie Mukhlis, Nurulafiqah Nadzirah Mansor, Hazlee Azil Illias, Lilik Jamilatul Awal, Li Wang, "New trends and future directions in load frequency control and flexible power system: A comprehensive review", *Alexandria Engineering Journal*, Volume 71, 2023, Pages 263-308, ISSN 1110-0168,
- [17]. M.H. Soliman, H.E.A. Talaat, M.A. Attia, "Power system frequency control enhancement by optimization of wind energy control system", *Ain Shams Eng. J.* 12 (4) (Dec. 2021) 3711– 3723, <https://doi.org/10.1016/J.ASEJ.2021.03.027>
- [18]. M. Beus and H. Pandzic, "Application of model predictive control algorithm on a hydro turbine governor control," 20th Power Syst. Comput. Conf. PSCC 2018, pp. 1–7, 2018, doi: 10.23919/PSCC.2018.8442594.
- [19]. Ram Babu, N., Bhagat, S.K., Saikia, L.C. et al. A Comprehensive Review of Recent Strategies on Automatic Generation Control/Load Frequency Control in Power Systems. *Arch Computat Methods Eng* 30, 543–572 (2023). <https://doi.org/10.1007/s11831-022-09810-y>
- [20]. Mohamed M. Ismail, Ahmed F. Bendary, Load Frequency Control for Multi Area Smart Grid based on Advanced Control Techniques, *Alexandria Engineering Journal*, Volume 57, Issue 4, 2018, Pages 4021-4032, ISSN 1110-0168, <https://doi.org/10.1016/j.aej.2018.11.004>.
- [21]. S.Prakash, S.K.Sinha, "Simulation based neuro-fuzzy hybrid intelligent PI control approach in fourarea load frequency control of interconnected power system," *Int. J. Applied Soft Computing*.23, 152–164, 2014.
- [22]. M. Osman, M. Elhaj and A. Salem, "Load Frequency Control in Two Area Power System using GA, SA and PSO Algorithms: A Comparative Study," 2021 31st Australasian Universities Power Engineering Conference (AUPEC), Perth, Australia, 2021, pp. 1-8, doi: 10.1109/AUPEC52110.2021.9597705.
- [23]. Mohammed Wadi, Abdulfetah Shobole, Wisam Elmasry, Ismail Kucuk, "Load frequency control in smart grids: A review of recent developments, *Renewable and Sustainable Energy Reviews*", Volume 189, Part A, 2024, 114013, ISSN 1364-0321,
- [24]. A Khodabakhshian and R Hooshmand. A new pid controller design for automatic generation control of hydro power systems. *International Journal of Electrical Power & Energy Systems*, 32(5):375–382, 2010.
- [25]. Asghar R, Riganti Fulginei F, Wadood H, Saeed S. A Review of Load Frequency Control Schemes Deployed for Wind-Integrated Power Systems. *Sustainability*. 2023; 15(10):8380. <https://doi.org/10.3390/su15108380>
- [26]. P.Bhatt, R.Roy, S.P.Ghoshal, "GA/particle swarm intelligence based optimization of two specific varieties of controller devices applied to two-area multi-units automatic generation control," *Int. J. Electrical Power & Energy Systems*.32, 299-310, 2010.
- [27]. M. M. Sati, D. Kumar, A. Singh, M. Raparathi, F. Y. Alghayadh and M. Soni, "Two-Area Power System with Automatic Generation Control Utilizing PID Control, FOPID, Particle Swarm Optimization, and Genetic Algorithms," 2024 *Fourth International Conference on Advances in Electrical, Computing, Communication and Sustainable Technologies (ICAECT)*, Bhilai, India, 2024, pp. 1-6, doi: 10.1109/ICAECT60202.2024.10469671

- [28]. Ram Babu, N., Bhagat, S.K., Saikia, L.C. *et al.* A Comprehensive Review of Recent Strategies on Automatic Generation Control/Load Frequency Control in Power Systems. *Arch Computat Methods Eng* **30**, 543–572 (2023). <https://doi.org/10.1007/s11831-022-09810-y>
- [29]. Feleke S, Pydi B, Satish R, Kotb H, Alenezi M, Shouran M. Frequency Stability Enhancement Using Differential-Evolution- and Genetic-Algorithm-Optimized Intelligent Controllers in Multiple Virtual Synchronous Machine Systems. *Sustainability*. 2023; 15(18):13892. <https://doi.org/10.3390/su151813892>
- [30]. Nicolaos et.al Munteanu, Iulian. Optimal Control of Wind Energy Systems, Towards a Global Approach. 01 2008
- [31]. Prabha S Kundur and Om P Malik. Power system stability and control. McGraw-Hill Education, 2022.
- [32]. Le-Ren Chang-Chien, Wei-Ting Lin, and Yao-Ching Yin. Enhancing frequency response control by dfigs in the high wind penetrated power systems. *IEEE transactions on power systems*, 26(2):710–718, 2010.
- [33]. H. K. Shaker, H. E. Zoghby, M. E. Bahgat and A. M. Abdel-Ghany, "Load Frequency Control for An Interconnected Multi Areas Power System Based on optimal Control Techniques," 2020 12th International Conference on Electrical Engineering (ICEENG), Cairo, Egypt, 2020, pp. 62-67, doi: 10.1109/ICEENG45378.2020.9171769.
- [34]. Gachhadar A, Maharjan RK, Shrestha S, Adhikari NB, Qamar F, Kazmi SHA, Nguyen QN. Power Optimization in Multi-Tier Heterogeneous Networks Using Genetic Algorithm. *Electronics*. 2023; 12(8):1795. <https://doi.org/10.3390/electronics12081795>.
- [35]. A. Gupta, R. P. Saini and M. P. Sharma, "Modeling of the hybrid energy system-Part I: Problem formulation and model development," *Renewable Energy*, vol. 36, no. 2, pp. 459–465, 2011.
- [36]. Feleke S, Pydi B, Satish R, Kotb H, Alenezi M, Shouran M. Frequency Stability Enhancement Using Differential-Evolution- and Genetic-Algorithm-Optimized Intelligent Controllers in Multiple Virtual Synchronous Machine Systems. *Sustainability*. 2023; 15(18):13892. <https://doi.org/10.3390/su151813892>